Article

Formation and Equilibrium of Ammonia in the Mg(NH)−2LiH Hydrogen Storage System

Yongfeng Liu, Jianjiang Hu, Guotao Wu, Zhitao Xiong, and Ping Chen

More About This Article

Additional resources and features associated with this article are available within the HTML version:

- Supporting Information
- Access to high resolution figures
- Links to articles and content related to this article
- Copyright permission to reproduce figures and/or text from this article

View the Full Text HTML

Formation and Equilibrium of Ammonia in the Mg(NH₂)₂−2LiH Hydrogen Storage System

Yongfeng Liu,[†,§] Jianjiang Hu,[†] Guotao Wu,[†] Zhitao Xiong,[†] and Ping Chen*,[†,‡]

Department of Physics, National University of Singapore, Singapore 117542, Singapore, and Department of Chemistry, National University of Singapore, Singapore 117543, Singapore

The equilibrium concentration of NH_3 in the volatile products of the reaction between $Mg(NH_2)_2$ and 2LiH and the decomposition of $Mg(NH_2)_2$ and $LiNH_2$, respectively, depends strongly on the reaction temperatures. The enthalpy changes of NH_3 generation in the decomposition of $LiNH_2$ and $Mg(NH_2)_2$ are deduced from the slopes of van't Hoff plots to be ca. 43.4 and 40.8 kJ/mol, respectively. When 600 psi hydrogen pressure was applied, the corresponding enthalpy changes increased to ca. 54.2 and 50.5 kJ/mol, respectively. For the $Mg(NH_2)_2$−2LiH system, the enthalpy change of NH_3 generation in hydrogen desorption was calculated to be ca. 80.3 kJ/mol, which is substantially higher than those of the decomposition of $Mg(NH_2)_2$ and $LiNH_2$. When high H_2 pressure (higher than equilibrium pressure) was applied, the corresponding enthalpy change decreased to ca. 51.3 kJ/mol, which is close to that of the decomposition of $Mg(NH_2)_2$ under high H_2 pressure.

1. Introduction

The metal−N−H system has attracted considerable attention as a potential hydrogen storage candidate since Chen et al. reported in 2002 that lithium nitride/imide could reversibly absorb/desorb a large amount of hydrogen.[1] A lot of studies have been done on the mechanistic understanding and the development of new metal−N−H compounds, such as Li−Mg−N−H,[2−6] Li−Ca−N−H,[2] Mg−Na−N−H,[7] Li−Al−N−H,[8−10] and Li−B−N−H.[11,12] Among them, the Li−Mg−N−H system was regarded as one of the most promising hydrogen storage materials for practical application.[2−6] Xiong et al.[2] and Luo et al.[3] have reported that about 5.0 wt % hydrogen could be reversibly stored in this system with equilibrium desorption pressure higher than 20 bar at 180 °C through the following reaction:

$$Mg(NH_2)_2 + 2LiH \leftrightarrow Li_2MgN_2H_2 + 2H_2$$
$$\Delta H = 44.3 \text{ kJ/(mol of } H_2) \quad (1)$$
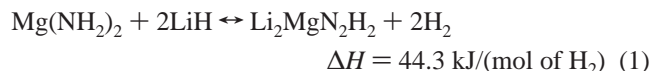
Further thermodynamic calculations indicated that hydrogen desorption from the Li−Mg−N−H system could be carried out at temperatures below 90 °C under 1.0 atm equilibrium H_2 pressure.[6]

In the dehydrogenation of $Mg(NH_2)_2$−2LiH, however, the thermal instability of $Mg(NH_2)_2$ would inevitably lead to its decomposition to MgNH and NH_3 at elevated temperatures according to reaction 2:

$$Mg(NH_2)_2 \rightarrow MgNH + NH_3 \quad (2)$$
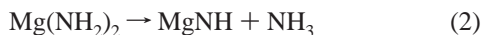
It is known that, for the polymer electrolyte membrane fuel cells (PEMFCs), a small amount of NH_3 present as an impurity in the fuel stream will lead to the loss of cell operating efficiency.[13] Furthermore, the decomposition of $Mg(NH_2)_2$ could induce a change in the chemical composition of the material which, consequently, will degrade the cycling hydrogen storage capacity. Therefore, it is of both practical importance and scientific interest to reveal the formation, concentration, and equilibrium of NH_3 during the hydrogen desorption process in Li−Mg−N−H systems.

Pinkerton has investigated the decomposition of $LiNH_2$, focusing on the kinetic aspect of the reaction.[14] Luo and co-workers[15] quantified the NH_3 concentration in the $Mg(NH_2)_2$−LiH system by using a Draeger tube (accuracy is ±15%). The results showed that NH_3 concentrations are ca. 180 ppm at 180 °C and 720 ppm at 240 °C, respectively, in a dynamic dehydrogenation. Little systematic elucidation on the thermodynamics of NH_3 formation in the Li−Mg−N−H system has been reported so far. In the present study, the decomposition of $LiNH_2$ and $Mg(NH_2)_2$ with and without external hydrogen pressure and their equilibrium NH_3 pressures have been measured by pressure−composition isotherms. Moreover, the equilibrium concentrations of NH_3 in the $Mg(NH_2)_2$−2LiH system during dehydrogenation and under high hydrogen pressure (higher than the desorption equilibrium pressure) have also been investigated. Reaction mechanisms under different reaction conditions are proposed and discussed.

2. Experimental Section

2.1. Sample Preparation. $LiNH_2$ (purity 95%) and LiH (purity >95%) were purchased from Aldrich and Fluka, respectively, and used as received. $Mg(NH_2)_2$ was synthesized in-house by reacting metallic Mg powder (99%, Riedel-De Haen) with 120 psi ammonia at about 300 °C; its structure was confirmed by X-ray diffraction (XRD) and the purity was ca. 98% determined by thermogravimetry. The $Mg(NH_2)_2$−2LiH sample was prepared by ball milling $Mg(NH_2)_2$ and LiH at a molar ratio of 1:2 at 200 rpm on a Retsch planetary ball mill (PM400) for 36 h. All samples were handled in a glovebox (MBRAUN) filled with purified argon to prevent contamination by air and moisture (H_2O < 1 ppm, O_2 < 1 ppm).

---

* Address correspondence to this author. Phone: +65 65165100. Fax: +65 67776126. E-mail: phychenp@nus.edu.sg.
† Department of Physics.
‡ Department of Chemistry.
§ Present address: Department of Materials Science and Engineering, Zhejiang University, Hangzhou 310027, People's Republic of China.
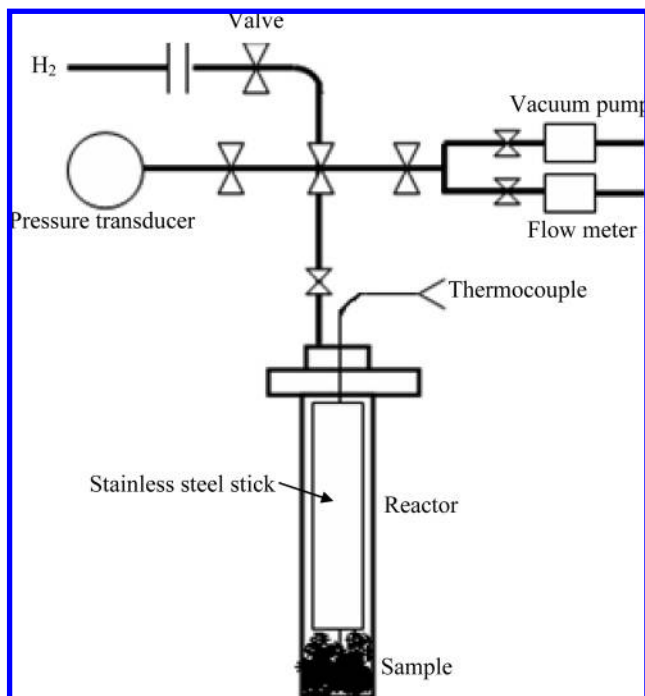
Figure 1. Schematic diagram of the high-pressure gas–solid reaction system.

Figure 2. TPD curves of the decompositions of $LiNH_2$ and $Mg(NH_2)_2$ with temperature.

2.2. TPD Measurement. The thermal decompositions of $LiNH_2$, $Mg(NH_2)_2$, and the post-milled $Mg(NH_2)_2-2LiH$ sample were monitored on a homemade temperature-programmed-decomposition (TPD) system. The TPD system is composed of a microreactor, a gas chromatograph (GC), and a mass spectrometer (MS). About 100 mg of sample was loaded and tested for each test. Purified Ar was used as carrier gas. The temperature ramping rate was 2 °C/min.

2.3. Measurements of NH_3 Concentration and Equilibrium Pressure. Hydrogen desorption isotherms of the $Mg(NH_2)_2-2LiH$ system were recorded on a self-constructed high-pressure gas–solid reaction apparatus (Figure 1). In order to observe the obvious change of the pressure inside the reactor with reacting and make the measurement more precise, a hollow stainless steel stick was used to minimize the tube reactor's vacant space. The tip of the thermocouple was inserted into the sample through the hollow stainless steel stick to obtain the actual reaction temperature. About 4.5 g of sample was loaded into the tube reactor, heated gradually to a prefixed temperature, and held there. Gaseous pressure was measured by a KELLER LEO RECORD transducer with a resolution of 0.1 bar. Sample temperature and the gaseous pressure in the reactor were monitored and recorded by a LabView-based software program. When hydrogen desorption reached equilibrium, the gaseous products were slowly introduced from the reactor to 30 mL of distilled water at a flux of 30 mL/min for 6 min. NH_3 gas was absorbed by the distilled water, and its concentration in distilled water was measured by a Metrohm 781 pH/ion meter (Switzerland) equipped with an NH_3-selective electrode. The measuring range of the model is 0.1 ppm to 1.7×10^4 ppm (NH_3), and its accuracy is ±10%. Standard aqueous solutions with known concentrations of NH_4Cl were used for the calibration, and the reliability of the measurement results was validated by 5% H_2-NH_3 mixed gas (volume ratio). The corresponding NH_3

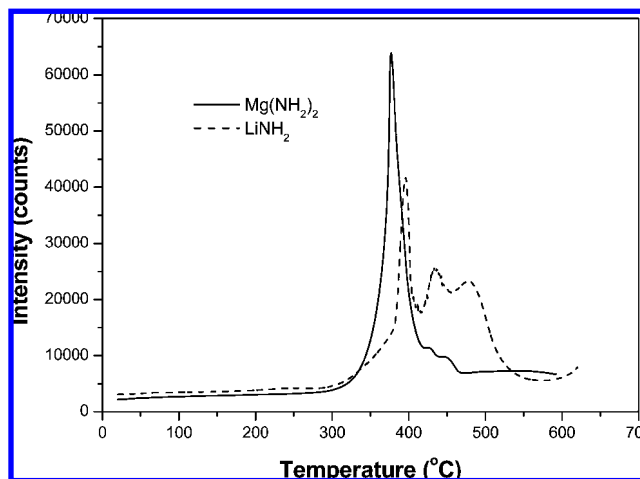concentration and partial pressure in the desorbed gases were calculated by the following equations:

$$C_{NH_3} = \frac{V_{H_2O}C'_{NH_3}/M_{NH_3}}{tr_f/22.4} \times 10^6 \qquad (3)$$

$$P_{NH_3} = PC_{NH_3} \qquad (4)$$

where C_{NH_3} is the concentration of NH_3 in the gaseous phase (ppm), C'_{NH_3} is the concentration of NH_3 in distilled water (ppm), V_{H_2O} is the volume of distilled water applied to absorb NH_3, M_{NH_3} is the molecular weight of NH_3, t is the time for gas collection (min), r_f is the rate of flux for gas collection (L/min), P_{NH_3} is the partial pressure of NH_3 in the gaseous mixture (psi), and P is the overall gaseous pressure in the reactor at a given temperature (psi). As ammonia is likely to be formed in both hydrogenation and dehydrogenation processes, two conditions were applied to track the origin of NH_3: (i) direct dehydrogenation of $Mg(NH_2)_2-2LiH$ at a given temperature until equilibrium was reached; (ii) exposing $Mg(NH_2)_2-2LiH$ to a hydrogen pressure which is higher than the desorption equilibrium pressure at a given temperature. The desorbed gases were collected at 167, 175, 184, 191, and 198 °C, respectively.

NH_3 equilibrium pressures in the decomposition of $LiNH_2$ and $Mg(NH_2)_2$ were also individually measured. About 4.5 g of sample was loaded into the tube reactor and gradually heated to and kept at the preset testing temperature until equilibrium was achieved. The NH_3 equilibrium pressures were obtained in the temperature ranges of 360–405 °C for $LiNH_2$ and 340–370 °C for $Mg(NH_2)_2$. Such high temperatures could prevent the adherence of NH_3 on the reactor inner walls and the stainless steel stick as well. To simulate the fully hydrogenated state of the $Mg(NH_2)_2-2LiH$ system, moreover, the decompositions of $LiNH_2$ and $Mg(NH_2)_2$ under high hydrogen pressure were also tested. A 600 psi hydrogen pressure, which is higher than the desorption equilibrium pressure of the $Mg(NH_2)_2-2LiH$ system at 200 °C, was applied. The NH_3 concentration in the gaseous phase was examined, and the corresponding NH_3 partial pressure was calculated by eqs 3 and 4.

3. Results and Discussion

3.1. TPD Behaviors. Figure 2 shows the TPD curves of the decomposition of $LiNH_2$ and $Mg(NH_2)_2$. It can be seen that the decomposition of $Mg(NH_2)_2$ started at ca. 300 °C and peaked at ca. 375 °C according to reaction 2. For $LiNH_2$, the NH_3
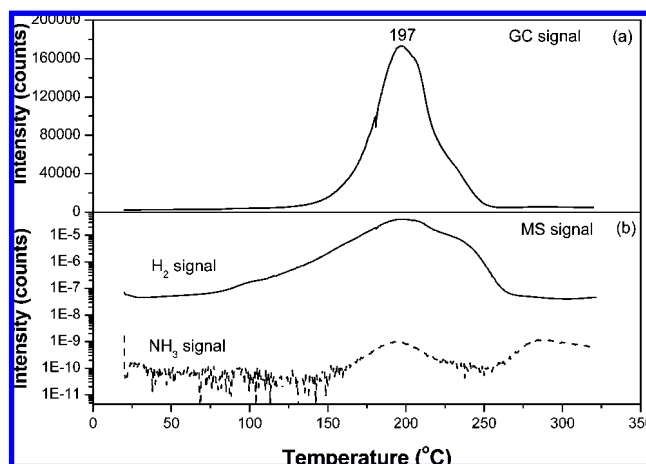
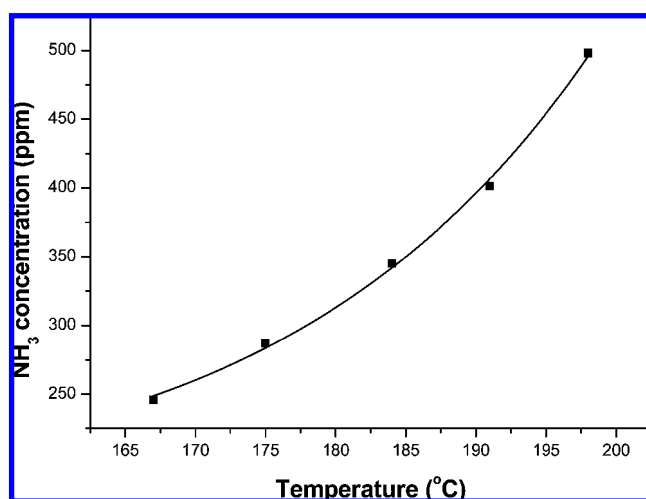**Figure 3.** TPD curve (a) and MS signals of H$_2$ and NH$_3$ (b) of the post-milled Mg(NH$_2$)$_2$−2LiH sample.

Figure 4. NH$_3$ concentration in the desorbed hydrogen of the Mg-(NH$_2$)$_2$−2LiH system at equilibrium state.

Figure 5. van't Hoff plot of NH$_3$ desorption from the Mg(NH$_2$)$_2$−2LiH system under hydrogen pressure higher than the equilibrium pressure.

Figure 6. van't Hoff plot of NH$_3$ desorption for the decomposition of LiNH$_2$ and Mg(NH$_2$)$_2$.

release also started at ca. 300 °C, but peaked at ca. 396 °C following reaction 5:

$$\mathrm{LiNH_2} \rightarrow \frac{1}{2}\,\mathrm{Li_2NH} + \frac{1}{2}\,\mathrm{NH_3} \qquad (5)$$
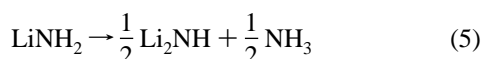
Figure 3 shows the TPD curve and MS signals of H$_2$ and NH$_3$ of the post-milled Mg(NH$_2$)$_2$−2LiH sample. As shown in Figure 3a, the starting temperature for gas desorption was ca. 100 °C, and the peak temperature was ca. 197 °C. MS analysis (Figure 3b) revealed that the main gaseous product was hydrogen. Traces of NH$_3$ were detected in the temperature range of 150−250 °C, but its intensity was much lower than those in the decomposition of LiNH$_2$ and Mg(NH$_2$)$_2$.

3.2. Equilibrium Concentration of NH$_3$ in Mg(NH$_2$)$_2$−2LiH. First, the equilibrium concentrations of NH$_3$ in the desorbed gases of the Mg(NH$_2$)$_2$−2LiH system were measured at 167, 175, 184, 191, and 198 °C, respectively. The results are shown in Figure 4 and Table 1. It can be seen that the NH$_3$ concentration increased monotonically with increasing temperature. The equilibrium concentration of NH$_3$ is ca. 240 ppm at 167 °C and 498 ppm at 198 °C. The NH$_3$ partial pressures in the desorbed gases were calculated using eq 4 and are presented in Table 1 and Figure 5 (solid circles). As shown in Figure 5, the plot of ln $P_{\mathrm{NH_3}}$ versus 1/T gives a straight line, showing a good van't Hoff relationship:[16]
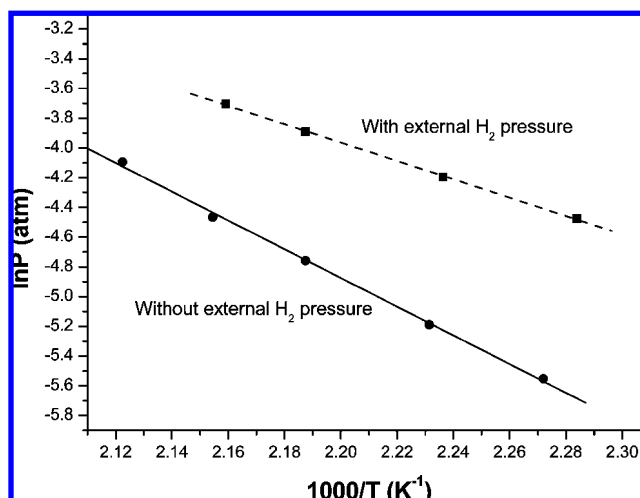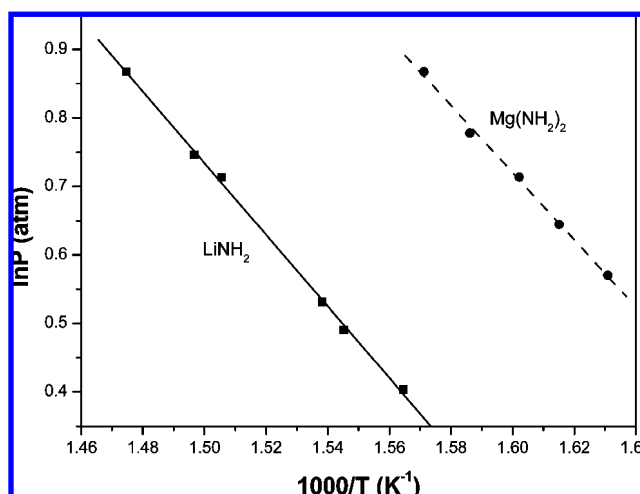
$$\ln P = -\frac{\Delta H}{RT} + \frac{\Delta S}{R} \qquad (6)$$

Here ΔH and ΔS are the enthalpy change (J/mol) and the entropy change (J/mol) of the reaction, respectively, T is absolute temperature (K), R is the gas constant, and P is the equilibrium pressure (atm). By fitting the data points in Figure 5, the van't Hoff equation for the NH$_3$ generation in reaction 1 was obtained as

$$\ln P = \frac{-9664}{T} + 16.4 \qquad (7)$$

Thus, the enthalpy change of NH$_3$ generation is ca. 80.3 kJ/mol (Table 2), which is close to the reaction heat of reaction 1.[6] Moreover, by extrapolating the straight line in Figure 5, the equilibrium NH$_3$ concentrations at 90 and 25 °C are ca. 30 and 17 ppm, respectively.

On the other hand, we also detected the NH$_3$ generation from the Mg(NH$_2$)$_2$−2LiH system under hydrogen pressure higher than the desorption equilibrium pressure. In this case, H$_2$ in the Mg(NH$_2$)$_2$−2LiH system cannot be desorbed, which corresponds to the system under the fully hydrogenated state. The results are also shown in Figure 5 and Table 1. Apparently the equilibrium pressure of NH$_3$ under high hydrogen pressure

TABLE 1: NH₃ Concentration of the Li−Mg−N−H System at Various Operation Temperatures

| temp (°C) | P_{eq}(H₂) of Li−Mg−N−H system (psi) | P_{eq}(NH₃) of Mg(NH₂)₂ decomposition (psi) | | P_{eq}(NH₃) of LiNH₂ decomposition (psi) | | NH₃ concn in Li−Mg−N−H system (ppm) | | press. of NH₃ in Li−Mg−N−H system (psi) | |
		without external hydrogen press.	with 600 psi hydrogen press.	without external hydrogen press.	with 600 psi hydrogen press.	without external hydrogen press.	with external high hydrogen press.	without external hydrogen press.	with external high hydrogen press.
167	231	1.10	0.17	0.54	0.16	246	518	0.057	0.18
175	287	1.34	0.22	0.66	0.21	287	540	0.082	0.23
184	366	1.67	0.30	0.83	0.28	345	618	0.126	0.30
191	421	1.97	0.36	0.98	0.35	401	676	0.169	0.37
198	491	2.30	0.44	1.21	0.43	498	751	0.245	0.45

TABLE 2: Enthalpy Change and Entropy Change of NH₃ for Mg(NH₂)₂−2LiH, LiNH₂, and Mg(NH₂)₂ under Different Conditions

sample	testing condition	ΔH_{NH_3} (kJ/mol)	ΔS_{NH_3} (J/mol)
Mg(NH₂)₂−2LiH	without external hydrogen pressure	80.3	136.3
	hydrogen pressure > equilibrium pressure	51.3	79.8
LiNH₂	without external hydrogen pressure	43.4	71.5
	under 600 psi hydrogen	54.2	88.1
Mg(NH₂)₂	decomposition	40.8	70.6
	under 600 psi hydrogen	50.5	79.8

(higher than the desorption equilibrium pressure) is higher than that under the dehydrogenation state. By linearly fitting the data between ln P and $1/T$, the van't Hoff equation for the NH₃ generation of the Mg(NH₂)₂−2LiH system under high hydrogen pressure was determined as

$$\ln P = \frac{-6175}{T} + 9.6 \tag{8}$$

The corresponding enthalpy change is calculated to be ca. 51.3 kJ/mol, which is lower than that of NH₃ generation under the dehydrogenation condition (80.3 kJ/mol), indicating that the mechanisms of the NH₃ generation under these two conditions are different.

The previous investigations on the mechanism for the hydrogen desorption from the Mg(NH₂)₂−2LiH system revealed that the following reaction should take place in the plateau region:[17]

$$2\text{Mg(NH}_2)_2 + 4\text{LiH} \rightarrow \text{Li}_2\text{Mg}_2\text{N}_3\text{H}_3 + \text{LiNH}_2 + \text{LiH} + 3\text{H}_2 \tag{9}$$
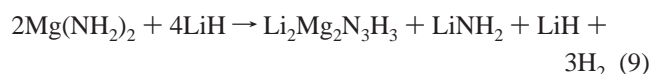
It was observed that LiNH₂ and Mg(NH₂)₂ coexisted in the system, and both of them may decompose to NH₃ at elevated temperatures. In order to identify the origin of NH₃, the equilibrium NH₃ pressure under the decomposition of LiNH₂ and Mg(NH₂)₂ was also measured.

3.3. Decomposition of LiNH₂ and Mg(NH₂)₂. Figure 6 shows the relationship between the NH₃ equilibrium pressure (P) and the operation temperature (T) for the decomposition of LiNH₂ and Mg(NH₂)₂. Obviously, ln P and $1/T$ also exhibit a good van't Hoff relationship, indicating that the decomposition of LiNH₂ and Mg(NH₂)₂ reached equilibrium at the given temperatures. The van't Hoff equations obtained for the decomposition of LiNH₂ (eq 10) and Mg(NH₂)₂ (eq 11) by fitting the data in Figure 6 are given below:

$$\ln P = \frac{-5226}{T} + 8.6 \tag{10}$$

$$\ln P = \frac{-4905}{T} + 8.5 \tag{11}$$

Calculated from eq 10, the enthalpy change of NH₃ generation by the thermal decomposition of LiNH₂ is ca. 43.4 kJ/mol, which is in good agreement with the theoretical value (42 kJ/mol) determined by the standard enthalpies of formation of LiNH₂ (−176 kJ/mol), Li₂NH (−222 kJ/mol), and NH₃ (−46 kJ/mol) for reaction 5.[18] For the thermal decomposition of Mg-(NH₂)₂, the enthalpy change is ca. 40.8 kJ/mol by eq 13, slightly smaller than that of LiNH₂.

To simulate the Mg(NH₂)₂−2LiH system under high H₂ pressure, the equilibrium NH₃ pressure in the decomposition of LiNH₂ and Mg(NH₂)₂ under 600 psi hydrogen was further measured and the corresponding ln P vs $1/T$ plots are shown in Figure 7. The van't Hoff equations of NH₃ generation in the decomposition of LiNH₂ and Mg(NH₂)₂ under 600 psi H₂ were derived as

$$\ln P = \frac{-6653}{T} + 10.6 \tag{12}$$

$$\ln P = \frac{-6079}{T} + 9.4 \tag{13}$$

In this case, the calculated enthalpy changes are ca. 54.2 and 50.5 kJ/mol for the decomposition of LiNH₂ and Mg(NH₂)₂
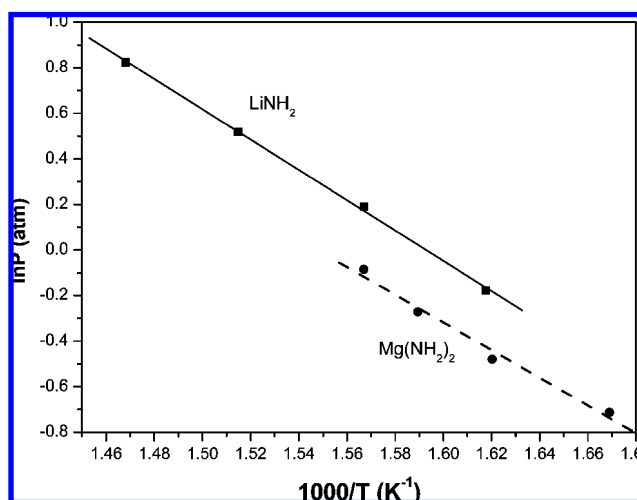
Figure 7. van't Hoff plot of NH₃ desorption for the decomposition of LiNH₂ and Mg(NH₂)₂ under 600 psi hydrogen pressure.

NH₃ in Mg(NH₂)₂−2LiH Hydrogen Storage System

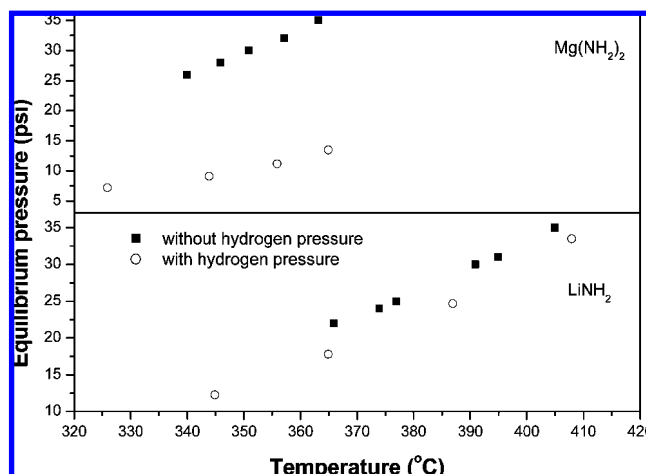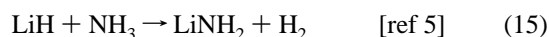*J. Phys. Chem. C, Vol. 112, No. 4, 2008* **1297**

Figure 8. NH$_3$ equilibrium pressure of the decomposition of LiNH$_2$ and Mg(NH$_2$)$_2$ with/without hydrogen pressure.

respectively, as shown in Table 2, which are obviously higher than those without addition of hydrogen (see Figure 8). This phenomenon indicates that the existence of hydrogen pressure in the reactor affects the decomposition of LiNH$_2$ and Mg-(NH$_2$)$_2$, suggesting that a more complicated reaction process than reactions 2 and 5 may exist. For the decomposition of LiNH$_2$ under high hydrogen pressure, reaction 5 should be the primary reaction and LiNH$_2$ was decomposed into Li$_2$NH and NH$_3$. Under hydrogen pressure, the Li$_2$NH could be hydrogenated into LiH and LiNH$_2$ according to the following reaction as reported in ref 1.

$$Li_2NH + H_2 \rightarrow LiH + LiNH_2 \qquad (14)$$
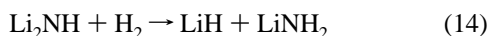
At the same time, the product of LiH can react with NH$_3$ by the following reaction:

$$LiH + NH_3 \rightarrow LiNH_2 + H_2 \qquad [\text{ref 5}] \qquad (15)$$

Apparently, the external hydrogen pressure can affect the self-decomposition of LiNH$_2$, and an equilibrium should have existed between reactions 5, 14, and 15 as the high hydrogen pressure was applied, which may be responsible for the NH$_3$ equilibrium pressure of the decomposition of LiNH$_2$ with external hydrogen pressure being lower than that without hydrogen pressure at the given temperature, as shown in Figure 8 and Table 1.

3.4. Possible Reaction Mechanism. By extrapolating the straight lines in Figures 6 and 7, the NH$_3$ equilibrium pressure in the decomposition of LiNH$_2$ and Mg(NH$_2$)$_2$ at low temperatures under different conditions could be obtained, and these are shown in Table 1. By comparison, the NH$_3$ equilibrium pressure in the dehydrogenation of Mg(NH$_2$)$_2$−2LiH is lower than those in the decomposition of LiNH$_2$ and Mg(NH$_2$)$_2$, which is due to the higher enthalpy change (ca 80.3 kJ/mol) for the NH$_3$ generation. Therefore, the NH$_3$ generation in the dehydrogenation of the Mg(NH$_2$)$_2$−2LiH system is not solely due to the decomposition of amide, but rather it could be a combined contribution from some parallel and/or competitive reactions existing in the reaction system. In the dehydrogenation plateau region of the Mg(NH$_2$)$_2$−2LiH system, four solid chemicals, Mg(NH$_2$)$_2$, LiH, LiNH$_2$, and Li$_2$Mg$_2$N$_3$H$_3$, can be observed as mentioned above. In addition to the primary reaction of reaction 9 for hydrogen desorption, Mg(NH$_2$)$_2$ and LiNH$_2$ may self-decompose to give out NH$_3$ according to reactions 2 and 5, respectively. Moreover, our investigation found that Li$_2$Mg$_2$N$_3$H$_3$

could also self-decompose and evolve NH$_3$ by the following reaction:

$$Li_2Mg_2N_3H_3 \rightarrow Li_2NH + \frac{2}{3} Mg_3N_2 + \frac{2}{3} NH_3 \qquad (16)$$
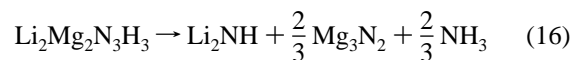
On the other hand, the emitted NH$_3$ can react with LiH according to reaction 15. Thus, it can be believed that the measured NH$_3$ concentration in the dehydrogenation of the Mg-(NH$_2$)$_2$−2LiH system should result from the reaction equilibrium of reactions 2, 5, 14, and 15. When high hydrogen pressure is applied, the enthalpy change of NH$_3$ generation in the Mg-(NH$_2$)$_2$−2LiH system (51.3 kJ/mol) is close to that of pure Mg-(NH$_2$)$_2$ (50.5 kJ/mol); therefore, the decomposition of Mg(NH$_2$)$_2$ is mainly responsible for the generation of NH$_3$ since the higher hydrogen pressure prevents the forward reaction of reaction 1 from proceeding.

4. Conclusion

The equilibrium concentrations of NH$_3$, the byproduct of the dehydrogenation reaction of Mg(NH$_2$)$_2$ and 2LiH, were determined at different temperatures. The results showed that the NH$_3$ generation depends strongly on the operation temperature. The equilibrium concentrations of NH$_3$ calculated at 90 and 25 °C are ca. 30 and 17 ppm, respectively. Moreover, the NH$_3$ equilibrium partial pressure in the Mg(NH$_2$)$_2$−2LiH system is obviously lower than that of the decomposition of LiNH$_2$ and Mg(NH$_2$)$_2$. Further calculations on the enthalpy changes show that it is ca. 80.3 kJ/mol for the NH$_3$ generation in the Mg-(NH$_2$)$_2$−2LiH system, considerably higher than those of the decomposition of LiNH$_2$ and Mg(NH$_2$)$_2$. All these results indicate that, for the isothermal dehydrogenation of Mg(NH$_2$)$_2$ and 2LiH, the NH$_3$ generation should be controlled by a set of reactions. On the other hand, the enthalpy change of NH$_3$ generation in the fully hydrogenated Mg(NH$_2$)$_2$−2LiH system is ca. 51.3 kJ/mol, very close to the value of the decomposition of Mg(NH$_2$)$_2$ under high hydrogen pressure (50.5 kJ/mol), indicating that the decomposition of Mg(NH$_2$)$_2$ under high hydrogen pressure is likely to be the dominant source for the NH$_3$ formation.

References and Notes

(1) Chen, P.; Xiong, Z. T.; Luo, J. Z.; Lin, J. Y.; Tan, K. L. *Nature* **2002**, *420*, 302.
(2) Xiong, Z. T.; Wu, G. T.; Hu, J. J.; Chen, P. *Adv. Mater.* **2004**, *16*, 1522.
(3) Luo, W. F. *J. Alloys Compd.* **2004**, *381*, 28.
(4) Leng, H. Y.; Ichikawa, T.; Hino, S.; Hanada, N.; Isobe, S.; Fujii, H. *J. Phys. Chem. B* **2004**, *108*, 8763.
(5) Leng, H. Y.; Ichikawa, T.; Hino, S.; Nakagawa, T.; Fujii, H. *J. Phys. Chem. B* **2005**, *109*, 10744.
(6) Xiong, Z. T.; Wu, G. T.; Hu, J. J.; Chen, P.; Luo, W. F.; Gross, K.; Wang, J. *J. Alloys Compd.* **2005**, *398*, 235.
(7) Xiong, Z. T.; Hu, J. J.; Wu, G. T.; Chen, P. *J. Alloys Compd.* **2005**, *395*, 209.
(8) Xiong, Z. T.; Wu, G. T.; Hu, J. J.; Chen, P. *J. Power Sources* **2006**, *159*, 167.
(9) Lu, J.; Fang, Z. Z. *J. Phys. Chem. B* **2005**, *109*, 20830.
(10) Kojima, Y.; Matsumoto, M.; Kawai, Y.; Haga, T.; Ohba, N.; Miwa, K.; Towata, S.; Nakamori, Y.; Orimo, S. *J. Phys. Chem. B* **2006**, *110*, 9632.

(11) Pinkerton, F. E.; Meisner, G. P.; Meyer, M. S.; Balogh, M. P.; Kundrat, M. D. *J. Phys. Chem. B* **2005**, *109*, 6.

(12) Pinkerton, F. E.; Meyer, M. S.; Meisner, G. P.; Balogh, M. P. *J. Phys. Chem. B* **2006**, *110*, 7967.

(13) Uribe, F. A.; Gottesfeld, S.; Zawodzinski, T. A., Jr. *J. Electrochem. Soc.* **2002**, *149*, A293.

(14) Pinkerton, F. E. *J. Alloys Compd.* **2005**, *400*, 76.

(15) Luo, W. F.; Stewart, K. *J. Alloys Compd.* **2007**, *440*, 357.

(16) Sandrock, G. *J. Alloys Compd.* **1999**, *293−295*, 877.

(17) Hu, J. J.; Liu, Y. F.; Xiong, Z. T.; Wu, G. T.; Chen, P. *J. Phys. Chem. C* **2007**, *111* (49), 18439.

(18) Aylward, G. H.; Findlay, T. J. V. *SI Chemical Data*, 4th ed.; John Wiley & Sons: Singapore, 1998.